Microwave Class-E Power Amplifiers

Zoya Popović and José A. García

Zoya Popović (Zoya.Popovic@colorado.edu) is with the Department of Electrical, Computer, and Energy Engineering, University of Colorado, Boulder, United States. José A. García (joseangel.garcia@unican.es) is with the Department of Communications Engineering, University of Cantabria, Santander, Spain.

Digital Object Identifier 10.1109/MMM.2018.2822202

Date of publication: 4 June 2018

 1527-3342/18©2018IEEE

Since Nathan Sokal's invention of the class-E power amplifier (PA), the vast majority of class-E results have been reported at kilohertz and millihertz frequencies, but the concept is increasingly applied in the ultrahigh-frequency (UHF) [1]–[13], microwave [14]–[20], and even millimeter-wave range [21]. The goal of this article is to briefly review some interesting concepts concerning high-frequency class-E PAs and related circuits. (The article on page 26 of this issue, "A History of Switching-Mode Class-E Techniques" by Andrei Grebennikov and Frederick H. Raab, provides a historical overview of class-E amplifier development.)

Frequency Scaling of the Class-E PA

Scaling class-E operation to higher frequencies presents a number of challenges. The most obvious is that the maximum frequency of class-E operation derived for the ideal class-E circuit is

$$f_{\max,E} \cong I_{\max}/(56.5 C_{\text{OUT}} V_{\text{ds}}), \tag{1}$$

where $I_{\max}$ is the maximum drain-to-source current of the switching device and V_{ds} its drain-to-source biasing voltage. The transistor output capacitance C_{OUT} limits the frequency range of class-E operation, as does the drain-to-source voltage, which implies lower output power. C_{OUT} can be de-embedded from a nonlinear model or measured large-signal parameters and used as a part of the output matching circuit. The class-E mode of operation is defined by the time-domain waveforms for a 50% duty cycle and assuming soft switching (both voltage and the derivative of the voltage are zero).

Assuming a high-Q output circuit and ideal bias choke, the current and voltage waveforms across the transistor can be derived, and the Fourier expansion can be used to find the theoretical impedance at the fundamental frequency:

$$Z_E = 0.28/(\omega C_{\text{OUT}}) e^{j49^\circ}. \tag{2}$$

This expression obtained from idealized circuit assumptions is the impedance at the transistor's virtual drain (current source); if this impedance is presented to a device, it will operate in class-E mode at frequencies governed by (1) and (2).

Designing an output circuit with an impedance Z_E at the switching frequency is a good starting point for design. The theory behind (2) assumes that all higher harmonics are open-circuited. At lower frequencies, this condition, along with a high-Q output circuit and a nearly ideal choke, can be implemented with lumped elements. However, in the UHF and microwave frequency range, lumped elements often have parasitics that limit the Q-factor and are difficult to predict. Conversely, distributed elements have lower loss and become sufficiently small.

Figure 1(a) shows a transmission-line implementation of a class-E PA with only the second harmonic termination [1]. The line and stub near the transistor output reference plane (at the current source) terminate the second harmonic in an open circuit and, together with the other two transmission lines, present Z_E from (2) at the fundamental frequency.

Active device internal parasitics are substantial at high frequencies and difficult to de-embed from nonlinear models, so the design of class-E waveforms at the virtual drain (where they are specified) poses a challenge. Additionally, the nonlinearity of the output capacitance affects the voltage and current time-domain waveforms and increases the voltage or current stress

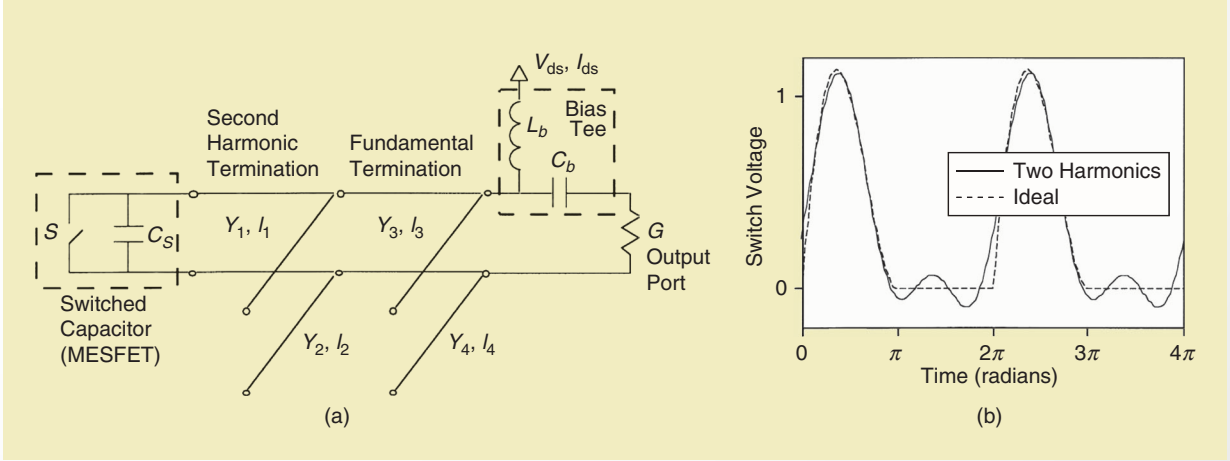

Figure 1. *(a) The transmission-line circuit topology for high-frequency class-E PAs with only the second harmonic open-circuited. (b) The associated switch voltage waveform. MESFET: metal–semiconductor field-effect transistor.*

The class-E mode of operation is defined by the time-domain waveforms for a 50% duty cycle and assuming soft switching (both voltage and the derivative of the voltage are zero).

on the device, lowering the output power, as shown in Figure 2 [48].

Another limitation is the device breakdown voltage, which needs to be at least 3.56 times the supply voltage for class-E operation; therefore, at high frequencies the output power is typically reduced. Other design challenges include input matching (switch control signal), bias line design, losses in the matching network, and low-frequency instabilities. Finally, the ideal class-E impedance given by (2) traces a counterclockwise loop on the Smith chart with increasing frequency, limiting class-E operational bandwidth.

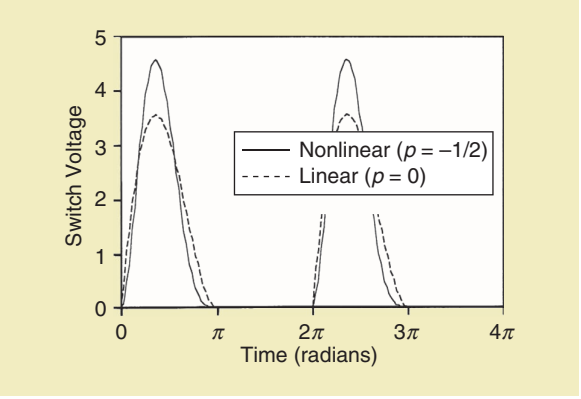

Figure 2. *When the device output capacitance is nonlinear [$p = -1/2$ is a square-root $C(V)$ nonlinearity], the voltage peak theoretically increases by 28% for this simple nonlinearity [48]. The vertical axis assumes a 1-V drain supply voltage, showing the increase of the peak compared to the $3.56V_D$ maximum swing for a linear output capacitance of the transistor C_{OUT}.*

UHF Class-E PAs

The standard series-resonant circuit at the output of a class-E PA, as proposed by Sokal, requires a high loaded Q-factor. But at UHF and low microwave frequencies, the parasitics associated with a high inductance value may result in self-resonance below the most significant higher-order harmonics, making proper harmonic terminations difficult [22]. A parallel resonant circuit tuned to provide an open condition at the second or third harmonic, or any convenient frequency between them, is shown in Figure 3(a) and discussed in [2].

A network that assures an impedance value closer to the optimum for both the second and third harmonics implements the parallel resonance with the coil's parasitic capacitance [3]. If the value is lowered to below the one that self-resonates between $2f$ and $3f$, its resistive losses may be reduced. The resulting lower Q-factor at the fundamental widens the bandwidth, while the degradation in efficiency may be negligible as long as the impedance at the most relevant harmonics remains high enough.

The output network is completed with a series reactance and a shunt capacitor to provide the optimum class-E termination at the fundamental. For the choke inductance L_b, a coil self-resonating at or near the fundamental may be selected and placed as in Figure 3(a) to avoid any undesired perturbation over the synthesized reactive terminations at $2f$ and $3f$.

Alternative lumped-element implementations, e.g., [4], have been derived from the frequency-domain transmission-line synthesis approach illustrated in Figure 1. The use of coils and capacitors has also been reported at UHF for other topologies in the continuum of class-E modes.

For any value of the dc-feed inductance L_b in Figure 3(b), optimum real and imaginary parts of the impedance at the fundamental satisfying zero-voltage switching (ZVS) and zero-voltage derivative switching conditions can be found [5] as a function of $q = 1/\sqrt{L_b \cdot C_{out}}$. Tracing a counterclockwise trajectory with frequency on a Smith chart, a simple *LCR* series network, like the one in Figure 3(b), may be adjusted to intercept it at two points, with the

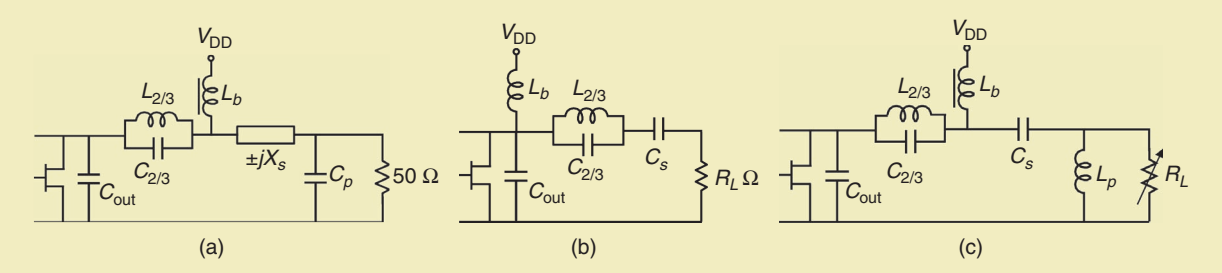

Figure 3. *The schematics of lumped-element topologies at the UHF band: (a) a wide-band class-E PA, (b) a continuous-mode class-E PA, and (c) a class-E PA for variable load operation.*

frequency spacing defining the bandwidth versus efficiency tradeoff [6]. The parallel resonant circuit would, in this case, play the same function as that described previously.

The original series-resonant topology is highly sensitive to load variations, and lumped-element networks that guarantee ZVS operation along a wide range of resistive loads have been proposed. In the UHF and low microwave bands, a few implementation solutions with load-insensitive operation have been demonstrated, based either on the addition of a transmission line equivalent network [7] or on the $q = 1.3$ case [8] of the continuous class-E space described in [5]. Figure 3(c) presents a slight modification to the topology in Figure 3(a), based on pioneering work with low-frequency metal-oxide-semiconductor (MOS) field-effect transistor (FET) class-E inverters [23]. An inductance-to-ground allows approximation of the optimum trajectory for efficient load modulation [9].

Examples of lumped-element UHF implementations of the previously discussed topologies are shown in Figures 3, 4, and 5. All are based on the Wolfspeed CGH35030F packaged gallium nitride (GaN) high-electron-mobility transistor (HEMT), using high-Q coils from Coilcraft's air core series and

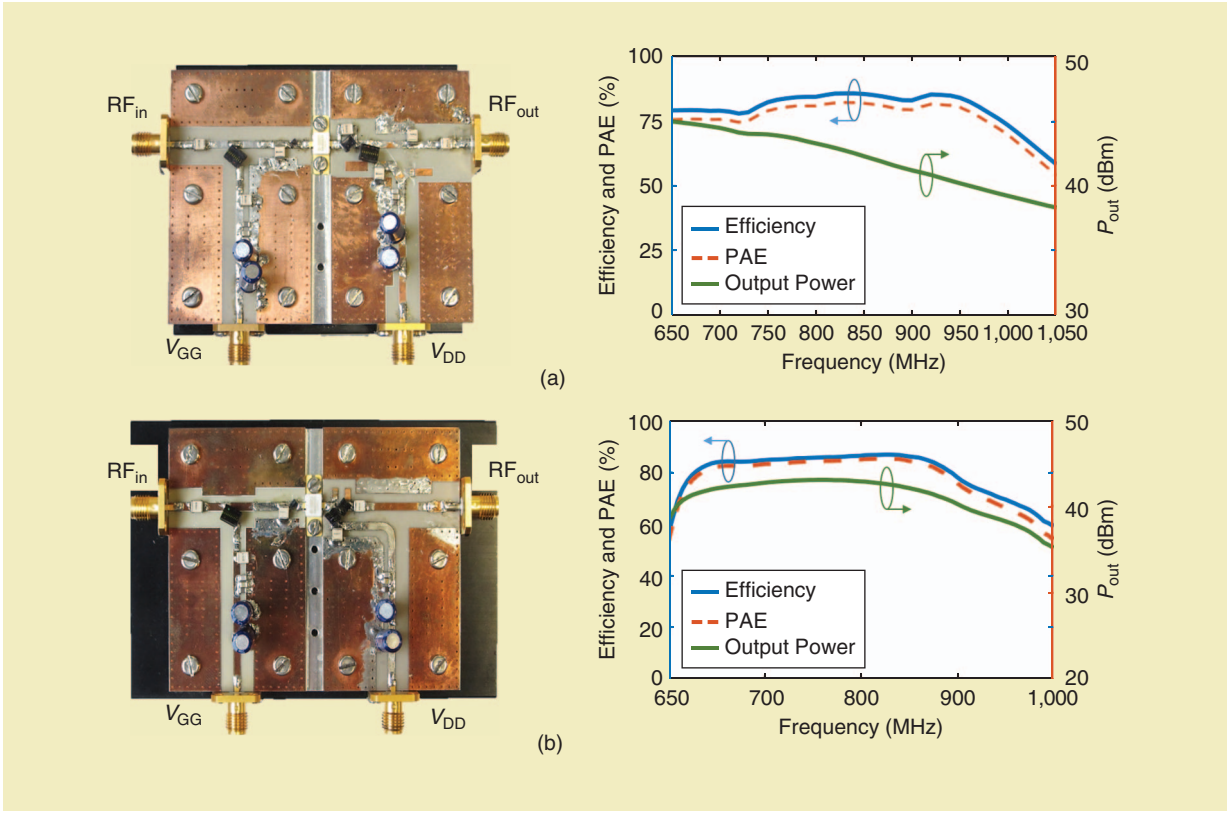

Figure 4. *(a) A wide-band lumped-element class-E PA in the 800-MHz UHF band (left) with the measured frequency response (right) [10]. (b) A wide-band continuous-mode class-E PA (left) and the measured frequency response (right) [6]. PAE: power-added efficiency.*

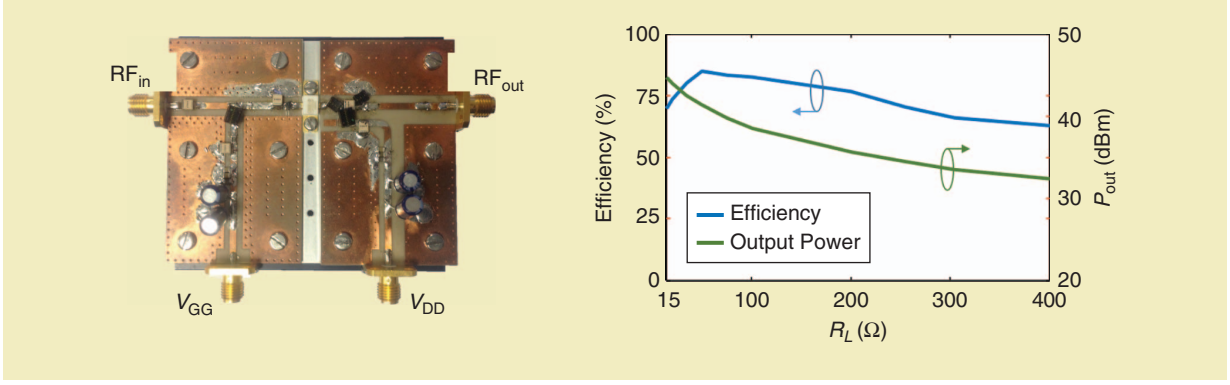

Figure 5. *A class-E PA for variable-load operation (left) with the measured results versus loading resistance (right) [9].*

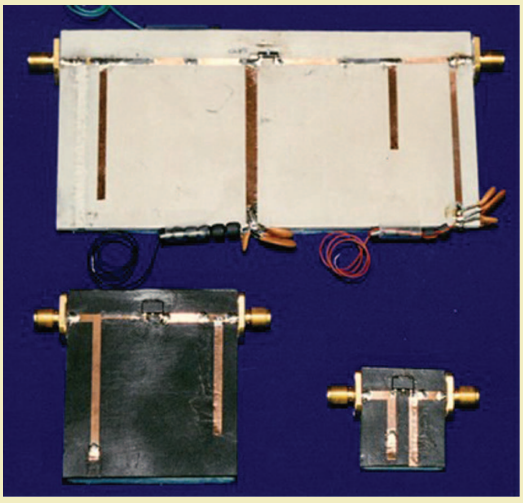

(a)

Frequency	0.5 GHz	1 GHz	2 GHz
$Gain_{meas}$	15.3 dB	14.7 dB	9.1 dB
PAE_{meas}	80%	73%	54%
$\eta_{D,theory}$	85%	73%	56%
$\eta_{D,meas}$	83%	75%	62%
$P_{out,theory}$	0.77 W	1.35 W	2.07 W
$P_{out,meas}$	0.55 W	0.94 W	0.53 W

(b)

Figure 6. *(a) A photo of first reported transmission-line 0.5-, 1-, and 2-GHz class-E PAs implemented with the CLY5 GaAs MESFET [1]. (b) A summary of measured and theoretically predicted performance.*

high-Q multilayer capacitors from American Technical Ceramics' 100B series. In the amplifier in Figure 4(a), the class-E operation is approximated over a wide bandwidth, trading resonant circuit Q-factors at the fundamental and second/third harmonics. A peak efficiency of 85.7% was measured and maintained above 80% over a 230-MHz frequency range (27% fractional bandwidth) with 4.2-dB of output power variation.

The dc-feed inductance in the PA shown in Figure 4(b) is carefully selected from commercially available values for continuous-mode class-E operation. The output capacitance of the CGH35030F transistor allows operation directly across a 50-Ω load in the desired frequency band. The parallel resonant circuit for the $2f$ and $3f$ terminations is provided by the parasitic capacitance of the coil in the output network. An efficiency value above 80% was measured for the 630–890-MHz frequency range (34% of fractional bandwidth) with a peak of 86.6%. The output power variation in that range is only 2.3 dB.

The amplifier in Figure 5 follows the schematic in Figure 3(c) for load-modulated but narrow-band ZVS

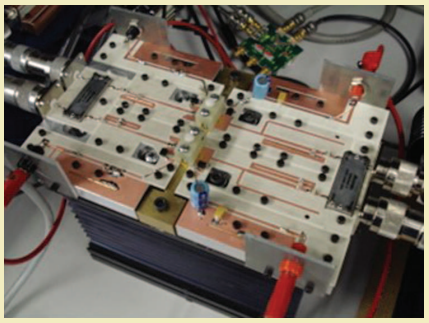

(a)

V_{DS} (V)	28	35	42
P_{out} (W)	50.8	75.2	99.8
Gain (dB)	15.7	17.1	18.6
η_D (%)	85	82	78.7
PAE (%)	83	81	77.6

P_{in} = 31 dBm, f = 370 MHz

(b)

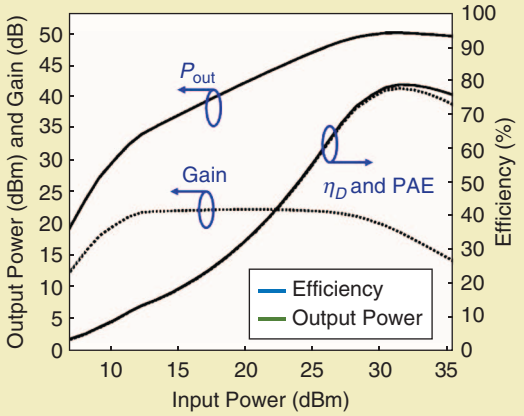

(c)

Figure 7. *(a) A photo of a 370-MHz hybrid class-E transmission-line PA with a GaN-on-SiC device from RFMD (RF3934, rated at 48 V with C_{OUT} = 18 pF, $R_{ON,DC}$ = 0.19 Ω, V_{TH} = −4.2 V). Note the N connectors for size. (b) The performance versus supply voltage for P_{in} = 31 dBm. (c) The measured amplifier continuous wave performance at 42-V drain supply [11].*

operation. With an 85% efficiency peak at 50-Ω loading condition, the measured efficiency was still as high as 70% at 10 dB of power backoff.

The first transmission-line implementations at 0.5, 1, and 2 GHz using a CLY5 gallium arsenide (GaAs) metal-semiconductor FET (MESFET) are shown in Figure 6 [1]. Here, the theoretical degradation with increasing frequency for a given device is demonstrated experimentally, and the circuits are designed analytically for first-pass success. Above 1 GHz, the device parameters do not satisfy (1), and the mode of operation first

becomes a suboptimal class-E mode, degrading into class-AB as the frequency increases further. The output power could not be well predicted due to inadequate nonlinear models in 1995.

Transmission-line class-E amplifiers have also been implemented at lower UHF frequencies when high output power levels might exceed the voltage/current handling of lumped components. A photo of such a class-E PA is shown in Figure 7 [11]. The 370-MHz PA is designed around a GaN-on-silicon carbide (SiC) HEMT and delivers 65 W with PAE of 82%, 45 W with PAE of 84%, and supply voltages of 35 and 28 V, respectively. Starting from class-E ideal impedance values, load pull under class-E conditions is used for device characterization and the matching network design. A weighted Euclidean distance is defined to enable tradeoff studies between output power and efficiency in achieving the final amplifier design [12].

In [12], class-E UHF PAs using four different devices are compared:

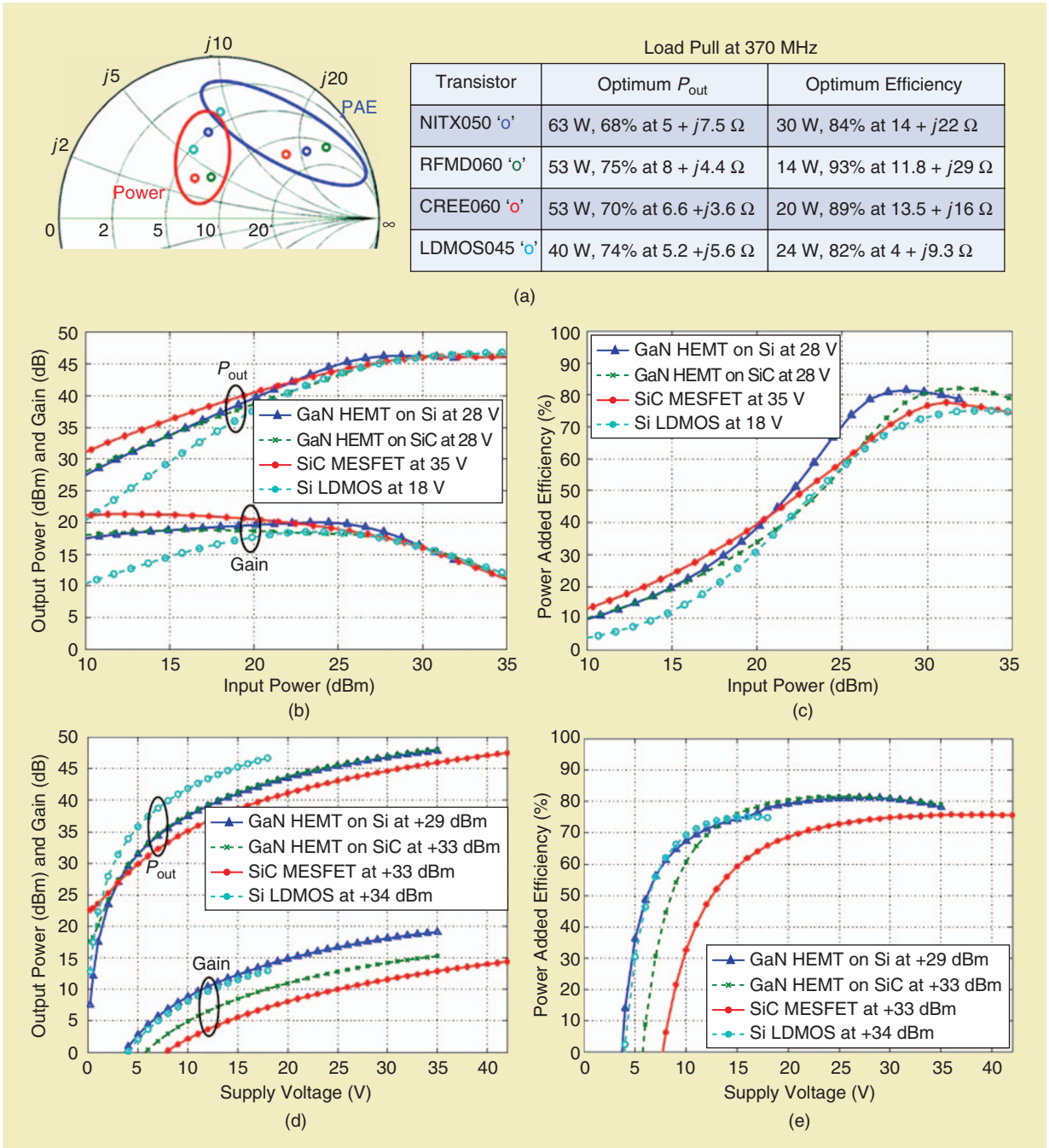

Figure 8. *(a) The load-pull data showing maximum output power and PAE points for the four devices (left) and the corresponding data (right). The measured output (b) power and gain and (c) PAE as a function of input power for the four types of devices. The measured (d) output power and gain and (e) PAE as a function of drain supply voltage.*

Active device internal parasitics are substantial at high frequencies and difficult to de-embed from nonlinear models, so the design of class-E waveforms at the virtual drain (where they are specified) poses a challenge.

1) Nitronex NPTB00050 (NITX050) GaN-on-Si HEMT (breakdown $V_{br} = 100$ V, $C_{out} = 9$ pF)
2) RF Micro Devices (RFMD) RF3932 (RFM060) GaN-on-SiC HEMT ($V_{br} = 150$ V, $C_{out} = 9$ pF)
3) Cree CRF24060 (CREE060) SiC MESFET ($V_{br} = 120$ V, $C_{out} = 11$ pF)
4) Agere AGR09045E (LDMOS045) Si laterally diffused MOS (LDMOS) ($V_{br} = 65$ V, $C_{out} = 23$ pF).

The PAs were all designed using ideal class-E equations as a starting point, and then a load pull was performed to determine the power-efficiency tradeoff.

The final results measured on all four PAs, including performance over supply voltage, are shown in Figure 8, demonstrating more than 45 W and greater than 80% efficiency in all cases, with the GaN HEMT amplifiers exhibiting the best overall performance in the UHF range (2008). A detailed comparison in terms of design parameters, amplitude modulation–amplitude modulation, and amplitude modulation–phase modulation performance, as well as performance over supply voltage, is presented in [12].

Microwave Class-E Amplifiers

A discussion of frequency scaling related to class-E performance up to the X-band is reviewed nicely in [13] and shown on example GaAs monolithic microwave integrated circuit (MMIC) and GaN hybrid PAs. A number of hybrid class-E amplifiers have been reported at the C-band, e.g., [14] and X-band [15]–[20] with GaAs FETs. MMIC class-E PAs are demonstrated in GaAs [13], [15], [20], indium phosphide (InP) [16], GaN [19], and complementary MOS (CMOS)/Si germanium (SiGe) [21], [24]. In 1998, a GaS MESFET (FLK052WG) class-E microstrip PA that delivers 0.61 W with a compressed gain of 9.8 dB, a drain efficiency of 81%, and a PAE of 72% at 5 GHz was integrated in a spatial combining array [14]. Antiresonant slot antennas were used to present the harmonic terminations.

More recently, several X-band GaAs class-E PAs have been demonstrated with PAE > 60%. Figure 9 provides an example in which a class-E PA stage is incorporated into a two-stage PA, with the first stage also operated in class-E mode, reaching a total PAE of 52% with a drain efficiency for the second stage of 62% [16].

Figure 10 shows a reconfigurable 10-GHz PA with an output matching network that enables the PA to operate in either linear class-A/AB or high-efficiency class-E using two Sandia microelectromechanical system (MEMS) ohmic switches. The insertion loss of

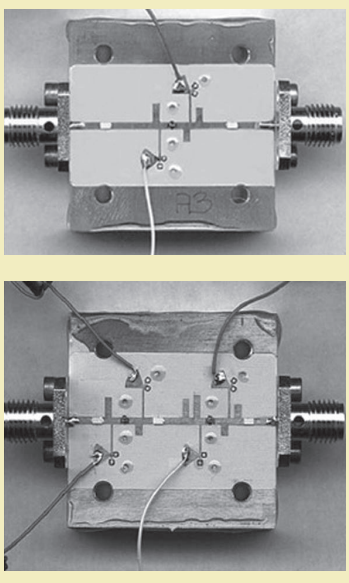

(a)

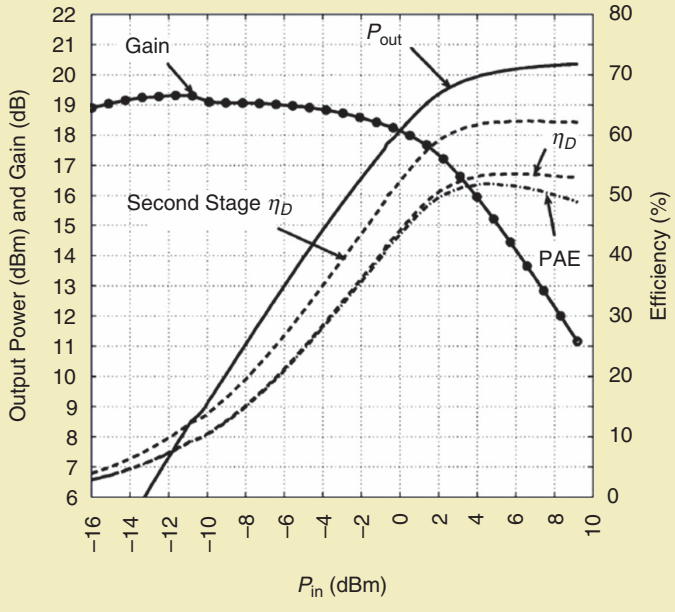

(b)

Figure 9. *(a) Photos of (top) the output stage only of a hybrid class-E 10-GHz GaAs PA with PAE of 62% and (bottom) a two-stage class-E PA with both stages operating close to the class-E condition. (b) The plots show the measured data for the two-stage PA calibrated at the subminiature-A connectors [16].*

the matching network in different states is below 0.3 dB, causing a few points of degradation in PAE compared to a nonreconfigurable static PA executed on the same alumina substrate and with the same GaAs MESFET die [18].

One of the first reported GaAs class-E X-band PAs is discussed in [15]. A photo of the single-stage MMIC along with its measured performance is presented in Figure 11, showing PAE of 65% at a power of 24 dBm. MMIC-integrated class-E PAs at the X-band include an InP two-stage amplifier, shown in Figure 12 [16], that had a measured PAE of 52% and compared well with the hybrid GaAs version in [16] in terms of efficiency points lost due to the first stage. In the case of two-stage class-E PAs [17], the interstage network can be designed to provide input harmonic waveshaping for a more squared waveform that controls the transistor operating as a switch.

More recently, several Si-based lower-power class-E PAs have been reported, in which the stacking of devices

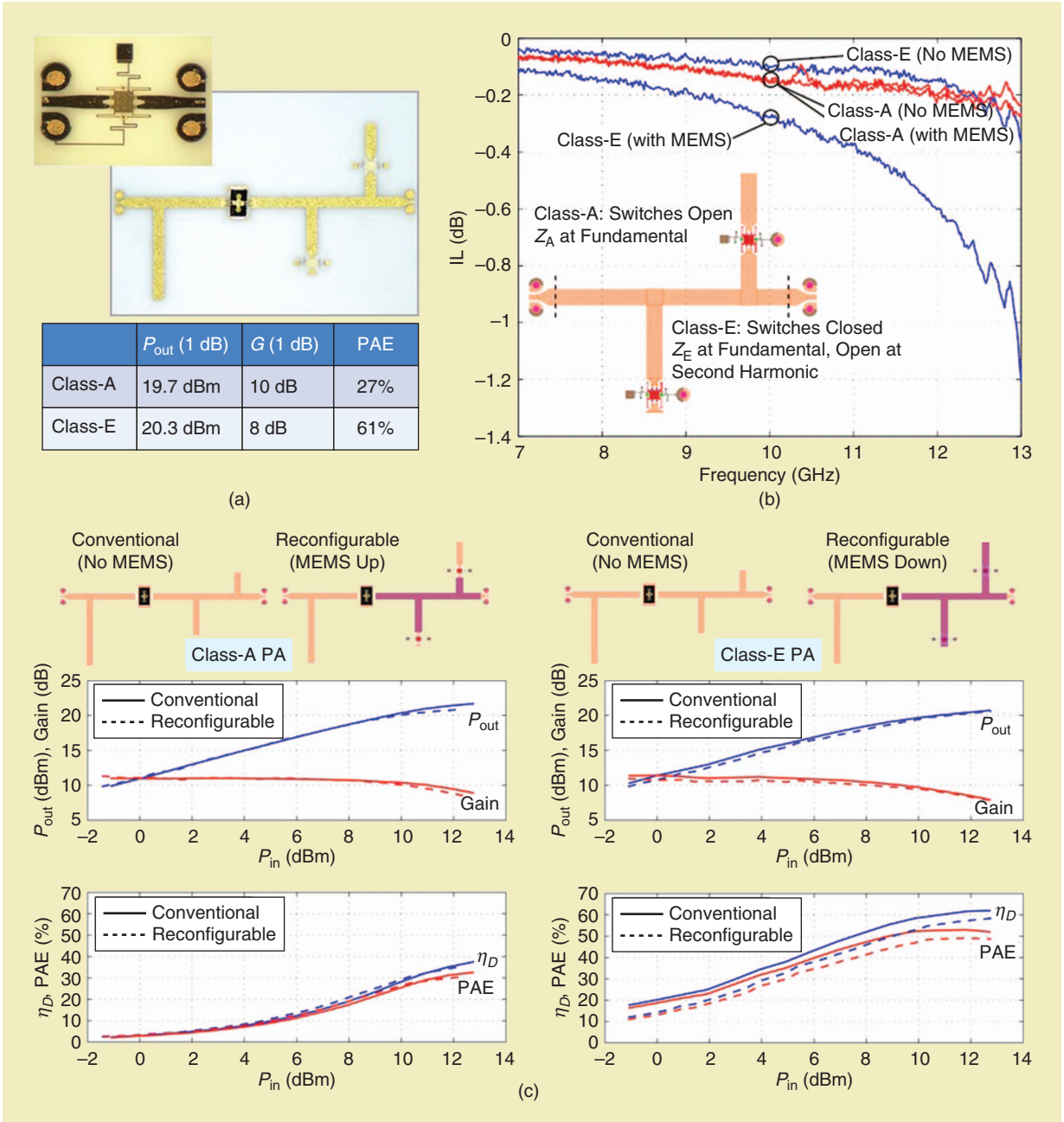

	P_{out} (1 dB)	G (1 dB)	PAE
Class-A	19.7 dBm	10 dB	27%
Class-E	20.3 dBm	8 dB	61%

Figure 10. *(a) A photo of a reconfigurable class-A/E PA with two MEMS switches [18] (top) and a table showing the performance parameters (bottom). (b) The plot shows the measured insertion loss of the matching networks with a degradation due to reconfigurability of, at most, 0.2 dB at 10 GHz. (c) The measured data in class-A (left) and class-E (right) modes for the 10-GHz mode-reconfigurable PA. The dashed lines show efficiency loss due to the reconfigurable MEMS network compared to a static class-E PA.*

is used to overcome the breakdown voltage limitation. In [24], a SiGe PA at 2.3–2.4 GHz demonstrated 62–65% efficiency using on-chip lumped elements, while in [25] a 5.3-GHz CMOS class-E PA showed PAE of 42% with a power density of 532 mW/mm^2. Other class-E PAs demonstrated in Si at lower microwave frequencies are exmined in, e.g., [26]–[32], with up to 1 W of output power level in the 1–2-GHz range. The millimeter-wave PA described in [21] demonstrates a CMOS IC at 93 GHz with PAE > 40%, showing that Sokal's class-E concept can be extended to extremely high frequencies (Figure 13).

Class-E PAs for High PAPR Signal Transmitters

Ideal class-E equations detailed in, e.g., [16] and [22] show that the output power across a fixed load is proportional to the square of the drain (collector) voltage,

$$P_{OUT} = 0.5\, R_E\, (1.86\, \pi\, \omega\, C_{OUT})^2\, V_{DD}^2, \quad (3)$$

which, in turn, implies that class-E PAs are very well suited to envelope tracking for efficiency improvement when the signal has a high peak-to-average power ratio (PAPR) [33]. Tracking using a class-E PA and a class-E dc–dc converter with excellent efficiencies in the 1-GHz range is demonstrated in [34]. The linearity of such an envelope-tracked transmitter is analyzed experimentally in [20] at a 10-GHz carrier with a two-tone signal. A two-stage 150-nm GaN-on-SiC PA is explained with the output stage designed using ideal class-E equations as a starting point and a power over 10 W, G_{sat} > 20 dB, and peak PAE > 60% [19], where the efficiency remains above 50% at 10-dB backoff. This PA was specifically designed for supply modulation, i.e.,

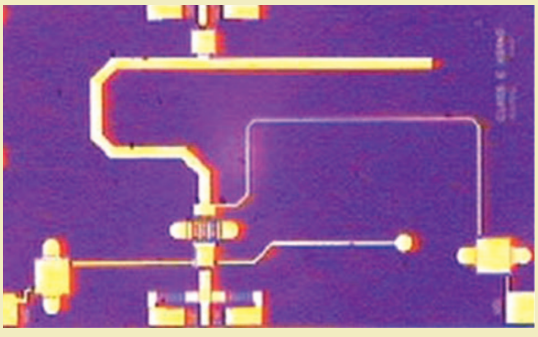

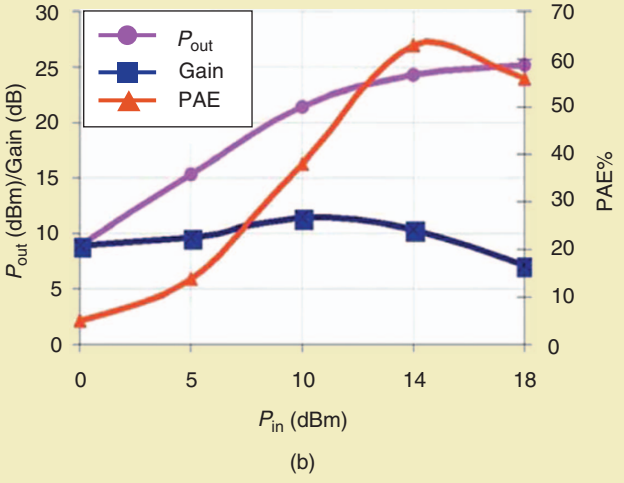

Figure 11. *(a) The GaAs MMIC PA from [15], (b) measured at 10.6 GHz.*

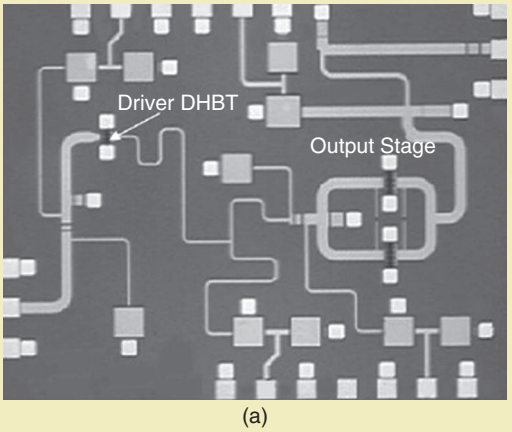

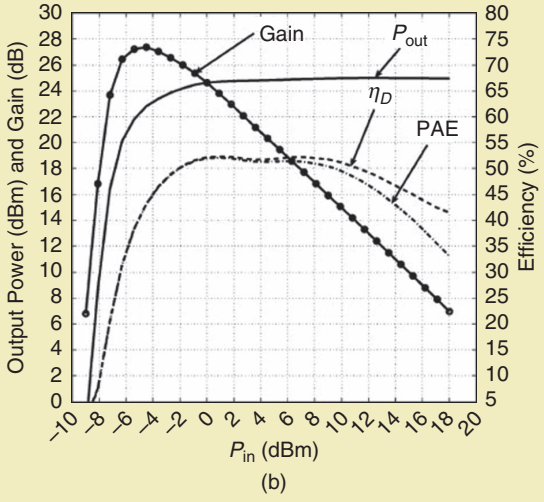

Figure 12. *(a) A photo of an InP two-stage PA MMIC and (b) the measured performance [16]. The MMIC is 2.65 mm × 2.1 mm. DHBT: double heterojunction bipolar transistor.*

to be stable with minimal capacitance in the drain bias line, enabling broadband signal transmission through the bias network. The measured efficiency curves are shown in Figure 14.

Another way to increase efficiency for high PAPR signals is via outphasing. It has been shown that class-E PAs lend themselves easily to a nonisolated (Chireix) architecture [7], [35]–[37].

The class-E PA is classically a tuned topology that, in practice, has approximately 10% bandwidth over which the frequency, power, and PAE remain close to the maximum. Extending the bandwidth of class-E PAs using a matching circuit design is investigated in, e.g., [38]–[40]. In [38], over 80% efficiency is obtained in a low-power class-E PAE from 1.7–2.7 GHz by input matching that includes second-harmonic optimization. In [39], the PAE exceeds 63% over the 0.9–2.2-GHz band, with 3-dB variation in output power. In [40], single-ended and differential matching networks are investigated to obtain a 1.7–2.2-GHz operational bandwidth with a class-E PA implemented in 90-nm CMOS operating in suboptimal mode, with efficiency over 42% and power above 25 dBm.

More recently, several Si-based lower-power class-E PAs have been reported, in which the stacking of devices is used to overcome the breakdown voltage limitation.

Conclusions

Other diverse aspects of class-E microwave circuits include oscillators, frequency multipliers, rectifiers, and dc–dc converters. The important issue of class-E amplifier stability is examined in [41], while [42] discusses the effects of parameter tolerances on class-E behavior. While rectifiers

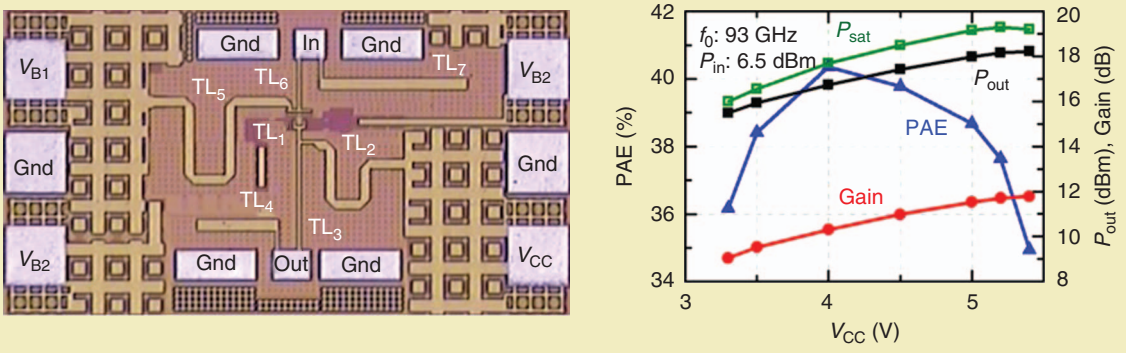

Figure 13. *(a) A photo of a bi-CMOS W-band class-E MMIC and (b) the measured performance [21]. Gnd: ground.*

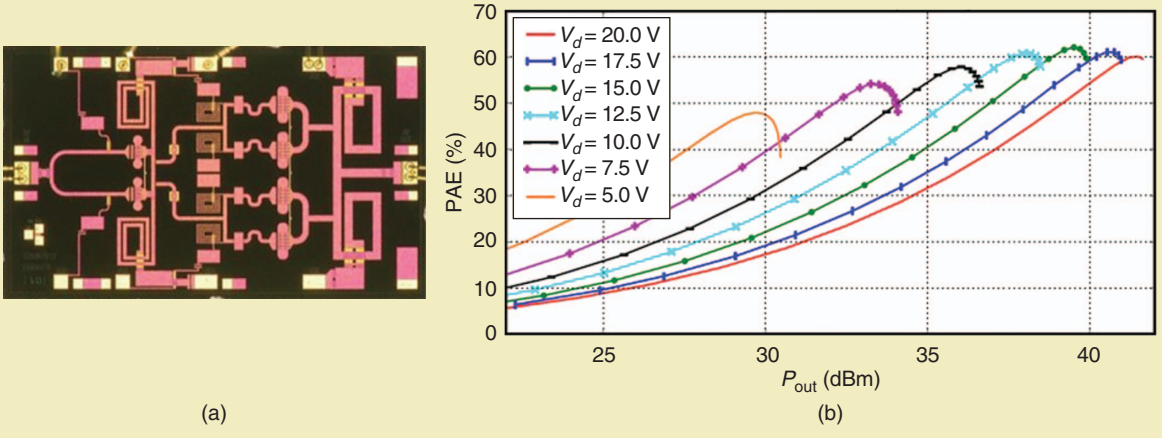

Figure 14. *(a) A10-GHz class-E MMIC PA for supply modulation [19]. The die is 3.8 mm × 2.3 mm, implemented in a 150-nm gate GaN-on-SiC process by Qorvo. (b) The measured PAE versus V_{dd} shows high efficiency up to 10-dB backoff, with a peak output power of 12 W and saturated gain over 20 dB [19].*

and dc–dc converters are a topic of a separate publication [43], Figures 15 and 16 show examples of microwave-frequency class-E oscillators [44], [45] and multipliers [46]. A class-E oscillating ring antenna at 10 GHz uses one mode of the ring as a directional coupler for feedback to a class-E amplifier and a different mode for radiation (Figure 15). This compact, efficient oscillator is a complete Doppler radar, because the gate bias controls the frequency of oscillation and the oscillator behaves as a self-oscillating mixer. Figure 16 offers a photo of a hybrid 10.4–20.8 class-E frequency doubler, along with time-domain waveforms and measured conversion gain and drain efficiency.

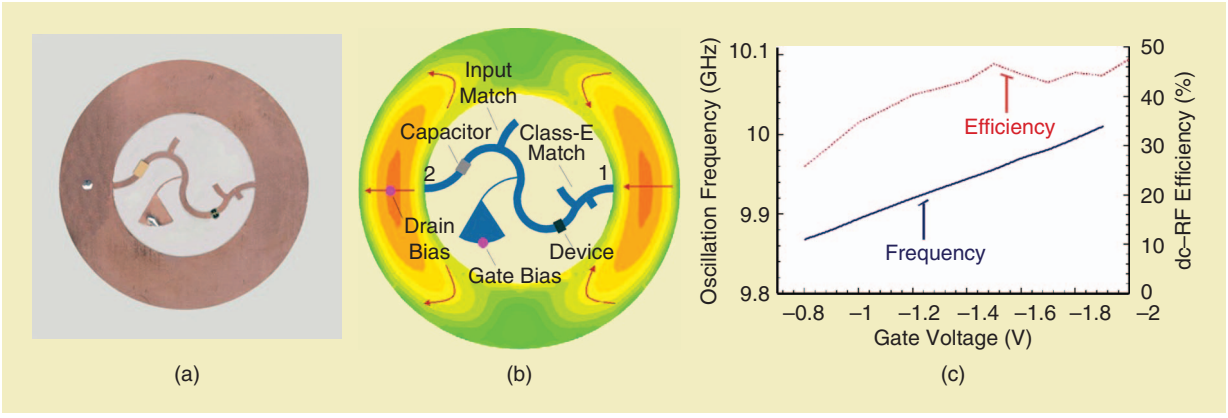

Figure 15. *A class-E active antenna oscillator implemented at 10 GHz with a GaAs MESFET. (a) A photo and (b) the circuit layout and current distribution on the antenna-coupler. (c) The measured conversion efficiency and output frequency as a function of gate bias. This integrated active antenna operates as a Doppler sensor because the class-E circuit is a self-oscillating mixer.*

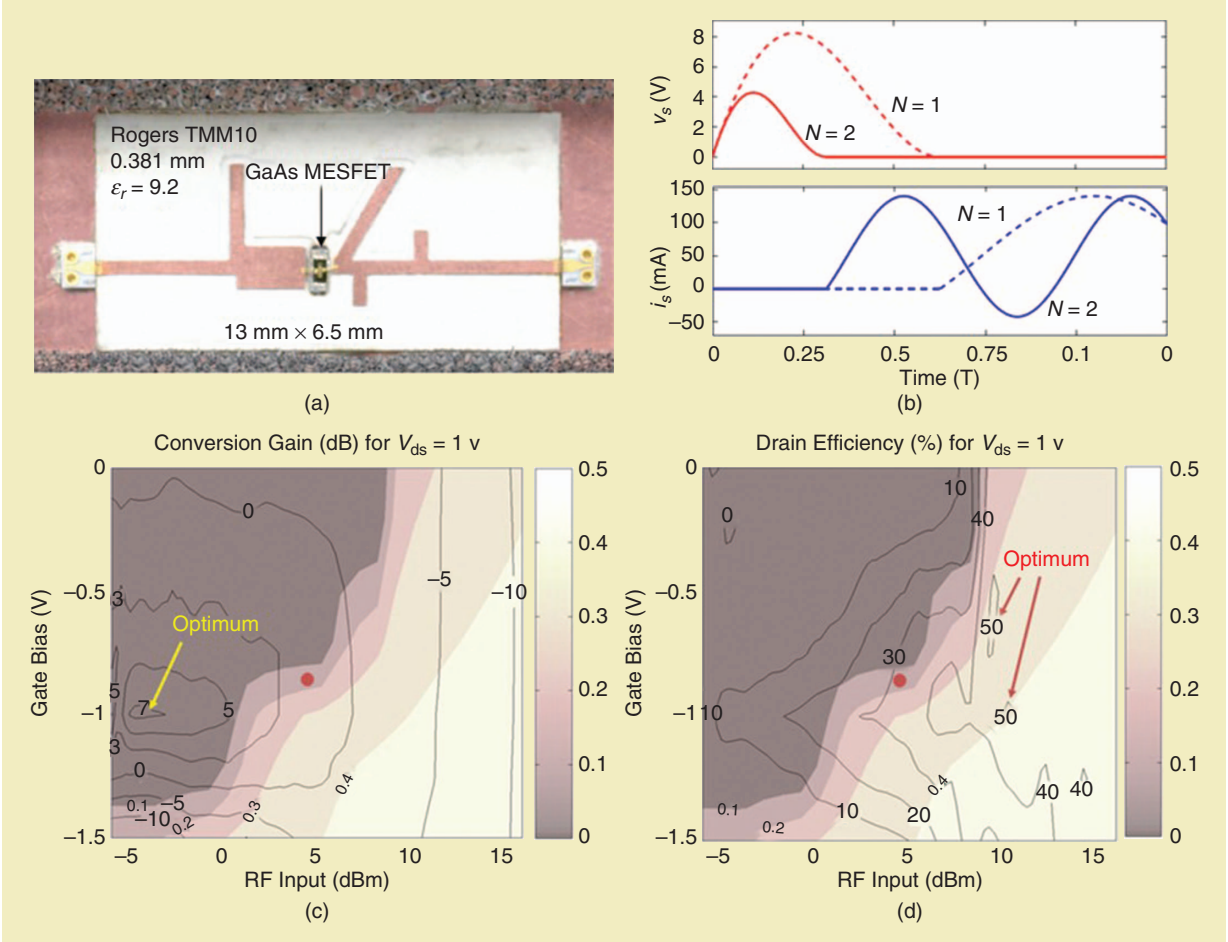

Figure 16. *(a) A photo of a class-E 10.4–20.8-GHz frequency doubler and (b) the time-domain waveforms. The measured (c) conversion gain (+7 dB at –3 dBm input) and (d) efficiency (50% at 10 dBm input) [46].*

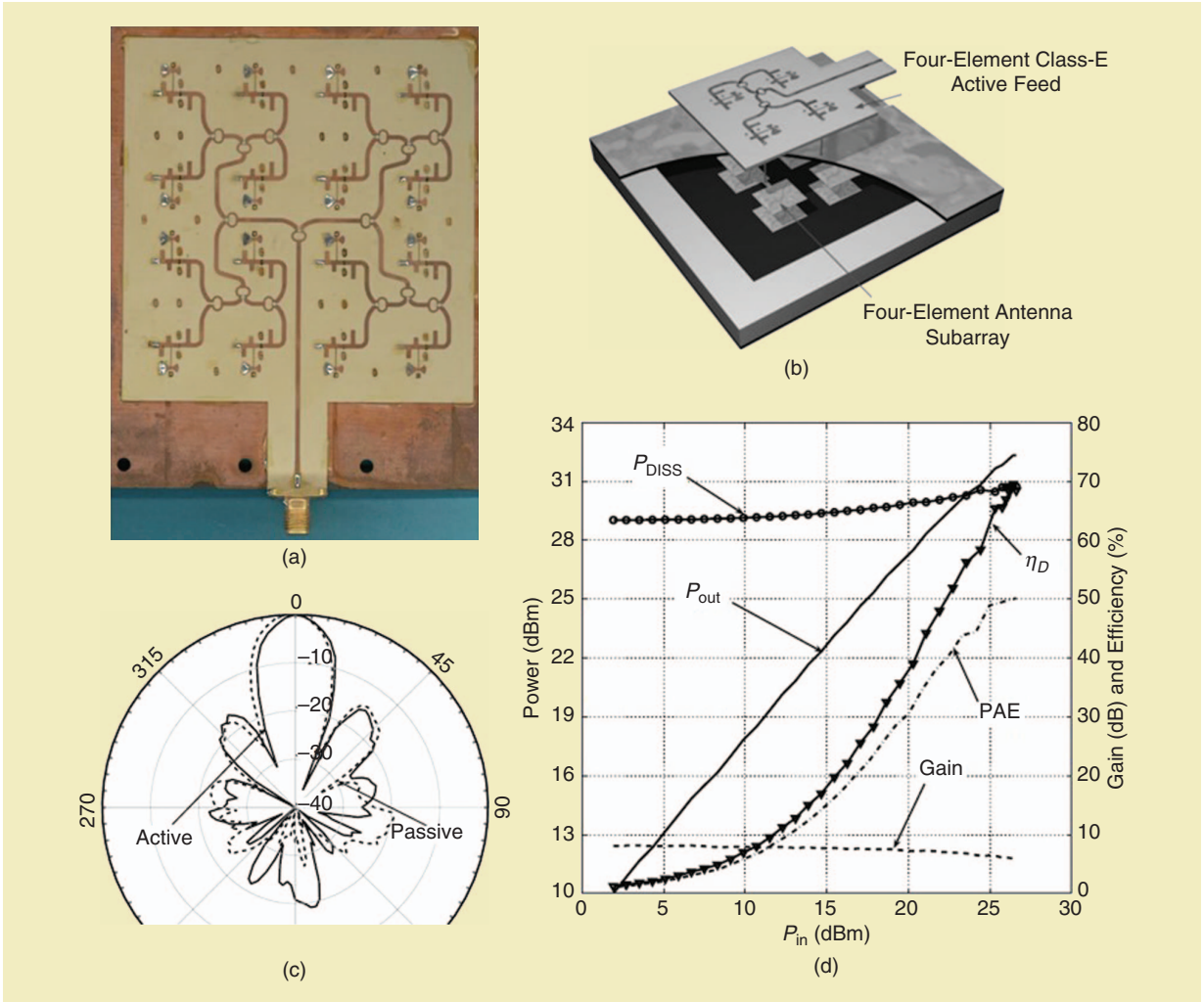

Figure 17. *(a) A photo of the corporate input network of a spatial power combiner with class-E PAs at 10 GHz [47]. (b) A sketch of the subarray, showing stacked patch antennas. (c) The measured E-plane radiation patterns of the passive and active arrays. (d) The measured array performance in a free-space configuration.*

Spatial power combining of 16 or more class-E PAs is demonstrated in [47]. Figure 17 shows the circuit side of an example 10-GHz array in which the 16 PAs are fed with a corporate Wilkinson combiner feed network, while the outputs are combined in free space upon radiation from a 16-element in-phase-fed patch-antenna array. The free-space combining efficiency is estimated to be 80%, which is higher than a four-level corporate network at 10 GHz.

In summary, we have presented a very brief overview that can provide only a glimpse into the vast area of microwave class-E PAs resulting from Nathan Sokal's pioneering work.

Acknowledgments

We acknowledge support, in part, by a Lockheed Martin Endowed Chair at the University of Colorado and in part by the Spanish Ministry of Economy, Industry, and Competitiveness (MINECO) through TEC2014-58341-C4-1-R and TEC2017-83343-C4-1-R projects, cofunded with FEDER.

References

[1] T. Mader and Z. Popovic, "The transmission-line high-efficiency class-E amplifier," *IEEE Guided Wave Lett.*, vol. 5, pp. 290–292, Sept. 1995.

[2] R. Negra and W. Bächtold, "Lumped-element load-network design for class-E power amplifiers," *IEEE Trans. Microwave Theory Tech.*, vol. 54, no. 6, pp. 2684–2690, June 2006.

[3] J. A. García, R. Marante, and M. N. Ruiz, "GaN HEMT class E^2 resonant topologies for UHF DC/DC power conversion," *IEEE Trans. Microwave Theory Tech.*, vol. 60, no. 12, pp. 4220–4229, Dec. 2012.

[4] R. Beltran and F. H. Raab, "Lumped-element output networks for high-efficiency power amplifiers," in *Proc. IEEE MTT-S Int. Microwave Symp.*, Anaheim, CA, 2010, pp. 324–327.

[5] M. Acar, A. J. Annema, and B. Nauta, "Analytical design equations for class-E power amplifiers," *IEEE Trans. Circuits Syst. I*, vol. 54, no. 12, pp. 2706–2717, Dec. 2007.

[6] M. N. Ruiz, A. L. Benito, J. R. Pérez-Cisneros, P. L. Gilabert, G. Montoro, and J. A. García, "Constant-gain envelope tracking in a UHF outphasing transmitter based on continuous-mode class-E GaN HEMT PAs," in *Proc. IEEE MTT-S Int. Microwave Symp.*, San Francisco, CA, 2016, pp. 1–4.

[7] R. Beltran, F. H. Raab, and A. Velazquez, "HF outphasing transmitter using class-E power amplifiers," in *Proc. IEEE MTT-S Int. Microwave Symp.*, Boston, MA, 2009, pp. 757–760.

[8] D. A. Calvillo-Cortes, M. P. van der Heijden, M. Acar, M. de Langen, R. Wesson, F. van Rijs, and L. C. N. de Vreede, "A package-integrated

Chireix outphasing RF switch-mode high-power amplifier," *IEEE Trans. Microwave Theory Tech.*, vol. 61, no. 10, pp. 3721–3732, Oct. 2013.
[9] D. Vegas, F. Moreno, M. N. Ruiz, and J.A. García, "Efficient class-E power amplifier for variable load operation," in *Proc. Integrated Nonlinear Microwave and Millimetre-Wave Circuits Workshop*, Graz, Apr. 2017, pp. 1–4.
[10] Z. Popović and J. A. García, "Microwave class-E power amplifiers," in *Proc. IEEE MTT-S Int. Microwave Symp.*, Honolulu, HI, 2017, pp. 1323–1326.
[11] N. D. Lopez, J. Hoversten, M. Poulton, and Z. Popovic, "A 65-W high-efficiency UHF GaN power amplifier," in *Proc. IEEE MTT-S Int. Microwave Symp. Digest*, Atlanta, GA, 2008, pp. 65–68.
[12] N. Lopez, "High-efficiency power amplifiers for linear transmitters," Ph.D. dissertation, Univ. Colorado, Boulder, 2008.
[13] P. Colantonio, F. Giannini, R. Giofre, M. A. Y. Medina, D. Schreurs, and B. Nauwelaers, "High frequency class E design methodologies," in *Proc. European GaAs/Semiconductor Application Symp.*, Paris, 2005, pp. 329–332.
[14] T. B. Mader, E. W. Bryerton, M. Markovic, M. Forman, and Z. Popovic, "Switched-mode high-efficiency microwave power amplifiers in a free- space power-combiner array," *IEEE Trans. Microwave Theory Tech.*, vol. 46, no. 10, pp. 1391–1398, Oct. 1998.
[15] R. Tayrani, "A monolithic X-band class-E power amplifier," in *Proc. 23rd IEEE GaAs IC Symp Digest*, Baltimore, MD, 2001, pp. 205–208.
[16] S. Pajic, N. Wang, P. Watson, T. Quach, and Z. Popovic, "X-band two-stage high-efficiency switched-mode power amplifiers," *IEEE Trans. Microwave Theory Tech.*, vol. 53, no. 9, pp. 2899–2907, Sept. 2005.
[17] R. Tayrani, "Two stage microwave Class E power amplifier." U.S. Patent 7 265 619, Sept. 4, 2007.
[18] P. J. Bell, Z. Popovic, and C. W. Dyck, "MEMS-switched class-A-to-E reconfigurable power amplifier," in *Proc. IEEE Radio and Wireless Symp.*, 2006, pp. 243–246.
[19] S. Schafer, M. Litchfield, A. Zai, Z. Popovíc, and C. Campbell, "X-band MMIC GaN power amplifiers designed for high-efficiency supply-modulated transmitters," in *Proc. IEEE MTT-S Int. Microwave Symp. Digest*, Seattle, WA, 2013, pp. 1–3.
[20] N. Wang, X. Peng, V. Yousefzadeh, D. Maksimovic, S. Pajic, and Z. Popovic, "Linearity of X-band class-E power amplifiers in EER operation," *IEEE Trans. Microwave Theory Tech.*, vol. 53, no. 3, pp. 1096–1102, Mar. 2005.
[21] P. Song, M. Oakley, A. C. Ulusoy, M. Kaynak, B. Tillack, G. Sadowy, and J. Cressler, "A class-E tuned W-band SiGe power amplifier with 40.4% power-added efficiency at 93 GHz," *IEEE Microwave Compon. Lett.*, vol. 25, no. 10, pp. 663–665, Oct. 2015.
[22] F. H. Raab, "Class-E, class-C, and class-F power amplifiers based upon a finite number of harmonics," *IEEE Trans. Microwave Theory Tech.*, vol. 49, no. 8, pp. 1462–1468, Aug. 2001.
[23] M. K. Kazimierczuk and X. T. Bui, "Class-E amplifier with an inductive impedance Inverter," *IEEE Trans. Ind. Electron.*, vol. 37, no. 2, pp. 160–166, Apr. 1990.
[24] D. Y. C. Lie, J. Lopez, J. D. Popp, J. F. Rowland, G. Wang, G. Qin, and Z. Ma, "Highly efficient monolithic class E SiGe power amplifier design at 900 and 2400 MHz," *IEEE Trans. Circuits Syst.*, vol. 56, pp. 1455–1466, July 2009.
[25] R. Brama, L. Larcher, A. Mazzanti, and F. Svelto, "A 30.5 dBm 48% PAE CMOS class-E PA with integrated balun for RF applications," *IEEE J. Solid-State Circuits*, vol. 43, no. 8, pp. 1755–1762, Aug. 2008.
[26] J. S. Walling, H. Lakdawala, Y. Palaskas, A. Ravi, O. Degani, K. Soumyanath, and D. J. Allstot, "A class-E PA with pulse-width and pulse-position modulation in 65 nm CMOS," *IEEE J. Solid-State Circuits*, vol. 44, no. 6, pp. 1668–1678, June 2009.
[27] J. S. Walling, S. S. Taylor, and D. J. Allstot, "A class-G supply modulator and class-E PA in 130 nm CMOS," *IEEE J. Solid-State Circuits*, vol. 44, no. 9, pp. 2339–2347, Sept. 2009.
[28] J. Chen, R. Bhat, and H. Krishnaswamy, "A compact fully integrated high-efficiency 5GHz stacked class-E PA in 65nm CMOS based on transformer-based charging acceleration," in *Proc. IEEE Compound Semiconductor Integrated Circuit Symp.*, La Jolla, CA, 2012, pp. 1–4.
[29] Y. Yamashita, D. Kanemoto, H. Kanaya, R. K. Pokharel, and K. Yoshida, "A CMOS class-E power amplifier of 40-% PAE at 5 GHz for constant envelope modulation system," in *Proc. IEEE 13th Topical Meeting on Silicon Monolithic Integrated Circuits in RF Systems*, Austin, TX, 2013, pp. 66–68.
[30] D. B. Santana, H. Klimach, E. Fabris, and S. Bampi, "A power controlled RF CMOS class-E PA with 43% maximum efficiency in 2.2 GHz," in *Proc. IEEE Int. Conf. Electronics, Circuits, and Systems*, Cairo, 2015, pp. 97–100.
[31] H. Alsuraisry, M. H. Wu, P. S. Huang, J. H. Tsai, and T. W. Huang, "5.3 GHz 42% PAE class-E power amplifier with 532 mW/mm^2 power area density in 180 nm CMOS process," *Electron. Lett.*, vol. 52, no. 15, pp. 1338–1340, July 2016.
[32] M. Kreißig, R. Kostack, J. Pliva, R. Paulo, and F. Ellinger, "A fully integrated 2.6 GHz cascode class-E PA in 0.25 μm CMOS employing new bias network for stacked transistors," in *Proc. IEEE MTT-S Latin America Microwave Conf.*, Puerto Vallarta, 2016, pp. 1–3.
[33] M. Weiss, F. Raab, and Z. Popovic, "Linearity of X-band class-F power amplifiers in high-efficiency transmitters," *IEEE Trans. Microwave Theory Tech.*, vol. 49, no. 6, pp. 1174–1179, June 2001.
[34] J. A. García, R. Marante, M. N. Ruiz, and G. Hernández, "A 1 GHz frequency-controlled class E^2 DC/DC converter for efficiently handling wideband signal envelopes," in *Proc. IEEE MTT-S Int. Microwave Symp. Digest*, Seattle, WA, 2013, pp. 1–4.
[35] M. N. Ruiz, A. L. Benito, J. R. Pérez-Cisneros, P. L. Gilabert, G. Montoro, and J. A. García, "Constant-gain envelope tracking in a UHF outphasing transmitter based on continuous-mode class-E GaN HEMT PAs," in *Proc. IEEE MTT-S Int. Microwave Symp.*, San Francisco, CA, 2016, pp. 1–4.
[36] D. A. Calvillo-Cortes, M. P. van der Heijden, M. Acar, M. de Langen, R. Wesson, F. van Rijs, and L. C. N. de Vreede,, "A package-integrated chireix outphasing RF switch-mode high-power amplifier," *IEEE Trans. Microwave Theory Tech.*, no. 10, pp. 3721–3732, Oct. 2013.
[37] A. Ghahremani, A. J. Annema, and B. Nauta, "A 20 dBm outphasing class-E PA with high efficiency at power back-off in 65 nm CMOS technology," in *Proc. IEEE Radio Frequency Integrated Circuits Symp.*, Honolulu, HI, 2017, pp. 340–343.
[38] V. Chaudhary and I. S. Rao, "A novel 2GHz highly efficiency improved class-E power amplifier for base stations," in *Proc. Int. Conf. Communication and Signal Processing*, Melmaruvathur, 2015, pp. 0940–0944.
[39] K. Chen and D. Peroulis, "Design of highly efficient broadband class-E power amplifier using synthesized low-pass matching networks," *IEEE Trans. Microwave Theory Tech.*, vol. 59, no. 12, pp. 3162–3173, Dec. 2011.
[40] M. D. Wei, D. Kalim, D. Erguvan, S. F. Chang, and R. Negra, "Investigation of wideband load transformation networks for class-E switching-mode power amplifiers," *IEEE Trans. Microwave Theory Tech.*, vol. 60, no. 6, pp. 1916–1927, June 2012.
[41] J. de Cos, A. Suárez, and J. A. García, "Hysteresis and oscillation in high-efficiency power amplifiers," *IEEE Trans. Microwave Theory Tech.*, vol. 63, no. 12, pp. 4284–4296, Dec. 2015.
[42] F. H. Raab, "Effects of circuit variations on the class E tuned power amplifier," *IEEE J. Solid-State Circuits*, vol. 13, no. 2, pp. 239–247, Apr. 1978.
[43] J. A. García and Z. Popović, "Class-E rectifiers and power converters," in *Proc. IEEE MTT-S Int. Microwave Symp.*, Honolulu, HI, 2017, pp. 1327–1330.
[44] E. W. Bryerton, W. A. Shiroma, and Z. B. Popovic, "A 5-GHz high-efficiency class-E oscillator," *IEEE Microwave Guided Wave Lett.*, vol. 6, no. 12, pp. 441–443, Dec. 1996.
[45] J. A. Hagerty and Z. Popovic, "A 10 GHz active annular ring antenna," in *Proc. IEEE Antennas and Propagation Society Int. Symp.*, 2002, pp. 284–287.
[46] M. Wiess, Switched-mode microwave circuits for high-efficiency transmitters," Ph.D. dissertation, Univ. Colorado, Boulder, 2001
[47] S. Pajic and Z. Popovic, "An efficient X-band 16-element spatial combiner of switched-mode power amplifiers," *IEEE Trans. Microwave Theory Tech.*, vol. 51, no. 7, pp. 1863–1870, July 2003.
[48] T. Mader, "Quasi-optical class-E power amplifiers," Ph.D. dissertation, Univ. Colorado, Boulder, 1995.